



Opportunities of desalination concentrates for lithium recovery: Optimal separation by synergic solvents

E. Fernández-Escalante, R. Ibañez, Ma.-F. San-Román *

Departamento de Ingenierías Química y Biomolecular, ETSIIyT, Universidad de Cantabria, Avda. de los Castros, 46, Santander 39005, Cantabria, Spain

ARTICLE INFO

Keywords:

Lithium
SWRO concentrates
Optimization
Response surface methodology

ABSTRACT

Lithium, highly demanded for its use in the battery industry, among other applications, has become a vulnerable commodity due to shortages in traditional sources. Although it is found in low concentration in SWRO brines, this waste represents a new source of this raw material. Based on previous studies in which Li^+ extractions $> 95\%$ were achieved, the optimal separation conditions of lithium from SWRO concentrates by solvent extraction with DBM•TOPO and FDOD•TOPO have been obtained for the first time. To this end, response surface methodology (RSM) with a three-level central composite design (CCD) has been applied. Three process variables, extractant concentration, basicity of the aqueous phase, and molar ratio between extractants, were evaluated using statistical parameters and second-order regression models. The optimized variables achieved maximum predicted extraction values of 99.7% for DBM•TOPO and 100% for FDOD•TOPO, not found yet in the open literature. Notably, for FDOD•TOPO system the needed pH for extraction is reduced, and both systems require a DBM:TOPO and FDOD:TOPO less than 1, a crucial consideration in terms of cost. This study opens new opportunities for lithium supply through desalination concentrates recovery.

1. Introduction

Over the past decades, the exponential increase in the world population and technological advances have given place to rising consumption of water, energy, and resources, in addition to waste generation [1]. To reduce the pressure on natural resources and generate sustainable growth, the European Commission adopted the new Circular Economy Action Plan (CEAP) in March 2020 [2]. This plan is one of the main components of the European Green Deal, and one of the six priorities of the Commission for the period 2019–2024 within the new European agenda for sustainable growth [2]. EU waste policy attempts to support the circular economy by extracting high-quality resources from waste and wastewater to the extent possible. In this direction, during the treatment of seawater in desalination plants, where volumes of around 79 million $\text{m}^3 \text{day}^{-1}$ are treated, concentrated wastewater streams (brines) with high added value are produced [3,4]. These concentrates, storing tons of minerals with almost all the elements of the periodic table [5,6], are a source of natural and economic wealth. Mineral recovery from brine rejected by seawater reverse osmosis (SWRO) desalination plants is getting more and more attention among the scientific community, as it aims to provide a new supply of valuable materials,

minimizing environmental damage produced by the exploitation of raw materials and the generation of waste [7,8].

In the available literature, it is possible to find numerous studies on the commercial recovery of the brines major cations (Na^+ , K^+ , Mg^{2+} and Ca^{2+}) in the form of NaCl, KCl, CaCO_3 or $\text{Mg}(\text{OH})_2$ [9–12], including patents and processes with high Technology Readiness Levels (TRL) [13–15]. In contrast, there are very few examples of the recovery of the minority elements that compose them [16]. Lithium is one of these elements, with concentrations lower than 2mg L^{-1} [17], significantly lower than those values reported in the literature for other non-conventional sources like salt lake brines of about 230–1500 mg L^{-1} . However, it is found in large quantities, if considering the amount of SWRO that is generated globally [18,19]. Specifically in Spain, in the Mediterranean Sea and Atlantic Ocean regions, currently a total of 437 desalination plants are producing freshwater, among them 35 are considered large or medium-sized treatment facilities ($\geq 25,000 \text{m}^3 \text{day}^{-1}$ of freshwater produced) [20]. This results in a flow of generated concentrates of $25,000 \text{m}^3 \text{day}^{-1}$ due to average recovery rate of 50% [21], so the potential amount of recoverable lithium from these concentrates would be up to 50kg day^{-1} in each desalination plant, amounting to at least 1750kg day^{-1} in total for Spain. This figure

* Corresponding author.

E-mail address: sanromm@unican.es (Ma.-F. San-Román).

<https://doi.org/10.1016/j.seppur.2023.124645>

Received 27 June 2023; Received in revised form 19 July 2023; Accepted 20 July 2023

Available online 21 July 2023

1383-5866/© 2023 The Authors. Published by Elsevier B.V. This is an open access article under the CC BY-NC-ND license (<http://creativecommons.org/licenses/by-nc-nd/4.0/>).

highlights the significant potential of obtaining substantial amounts of lithium from desalination plant concentrates, which is of great relevance in a context where the demand for lithium is constantly increasing due to its use in various strategic industries. In fact, global lithium consumption in 2022 reached 134,000 tons, a remarkable 41 % increase over the 95,000 tons consumed in 2021, in response to strong demand from the lithium-ion battery market and rising lithium prices [22–25]. It is in this context, where arises the necessity to intensify research on the development of efficient technologies for lithium recovery.

Until now, different studies have reported solvent extraction techniques as a potential process for the separation of lithium from seawater concentrates, due to the key advantages it offers, including its closed-loop nature that allows the recyclability of the extractants, reducing the need for constant replacement [9,26–28]. In previous works [29,30], we investigated the synergistic effect in extraction systems containing β -diketones and organophosphates. Through molecular simulation, using density functional theory (DFT), the thermodynamic and equilibrium parameters were determined for the previously selected extractants mixtures to separate lithium from the majority cations present in the brines Na^+ , K^+ , Mg^{2+} , Ca^{2+} and Sr^{2+} [29]. It was observed that the combinations DBM•TOPO and FDOD•TOPO provided the best selectivity results towards lithium. Subsequently, we conducted experimental work to confirm their feasibility [30]. In terms of extractant concentration, 0.06 M of DBM•TOPO (ratio 1:1) and 0.014 M of FDOD•TOPO (ratio 1:1) were required to achieve high lithium separation rates. In both cases, lithium extraction above 95 % was obtained under alkaline conditions ($\text{pH} \geq 12$ for DBM•TOPO and $\text{pH} \geq 10$ for FDOD•TOPO). The basic pH favors the tautomeric effect that occurs in β -diketones (formation of enolate groups) and with it the lithium extraction process [30]. Besides, it was demonstrated that by employing these extractants mixtures, the rest of the cations present in brines were not extracted, being obtained then selective separation of lithium from desalination concentrates. These findings provided the best results in the open literature related to the selective extraction of Li^+ in complex mixtures like SWRO desalination brines, in terms of selectivity and extraction percentage. A step further in the processes of separation with solvents entails the determination of the operating variables that make the separation the best possible, that is, the optimization of the process. For this, it is necessary to select the operation variables, and their value ranges, that influence significantly the separation. In this work, taking into account the previous experimental results, pH, extractant concentration and the molar ratio between extractants have been selected [29,30]. Given the large number of experiments that would be necessary to carry out, Response Surface Methodology (RSM) has been used, avoiding so, excessive time-consuming experimentation and costs, reaching, besides, more reliable and accurate results.

The use RSM in the Design of Experiments (DOE) is a competent method to reach optimum results with a minimum number of experiments [31,32]. RSM is a very important tool used by researchers to develop new processes, optimize performance, and improve the design of new products [33]. It is applied to model building, assessing the effects of different factors (operation variables) and finding the optimal conditions for the desired response through factorial design. Inside RSM, the Central Composite Design (CCD) is the most employed tool used to carry out the experiments design, as it is well suited for fitting a quadratic surface, ideal for sequential experimentation, allowing a reasonable amount of information to test for misfits without involving an unusually large number of design point [31]. Several studies have used RSM to optimize extraction processes. Dutta et al. [34] optimized the recovery of copper from printed circuit boards using RSM to study the effects of acid concentration, pulp density, temperature, and time, validating their extraction method for maximum Cu^{2+} recovery (99.99 %). Mohammad et al. [35] studied the optimization by RSM of magnesium recovery from desalination brines through reaction with ammonia, obtaining the optimal values of their study variables (brine salinity, reaction temperature and ammonia to magnesium molar ratio),

with a maximum rate of 99 % magnesium recovery. Katozi et al. [36] studied optimized zinc (II) solvent extraction using D2EHPA on a pilot scale, considering the effect of pH, reaction time and extractant volume ratio, achieving zinc extractions between 76 % and 93 %.

This research aims to optimize the selective lithium separation conditions, researched in previous studies, using the tools RSM and CCD. This optimization has been carried out using the combinations of DBM•TOPO and FDOD•TOPO as synergic solvents. Knowing that, extractant concentration, pH and the molar ratio between both β -diketones and TOPO are the main independent variables that influence effectively the lithium separation, a design of experiments has been performed for each solvent mixture in order to investigate the operating factors and most relevant levels that influence the extraction efficiency. These results are expected to provide the optimum operating conditions to maximize the separation of lithium from desalination concentrates, contributing to a sustainable approach to the desalination process of seawater and, in the long term, to recover valuable metals from brines and discharge low-salinity water, promoting a circular economy and minimizing environmental impact.

2. Materials and methods

2.1. Materials and instruments

Lithium chloride (LiCl , >99 %) was obtained from Labkem (Spain). Standard solution of 1000 mg/L of lithium was purchased from Agilent (CA, USA). Deionized water was generated using a Milli-Q ultrapure water purification system from Millipore. Ammonia (NH_3 , 25 %) was purchased from PanReac AppliChem (Spain). Kerosene (ShellSol D70) was obtained from Kremer (Germany). Extractants dibenzoylmethane (DBM, 98 %) and trioctylphosphine oxide (TOPO, 99 %) were acquired from Acros Organics (China and Japan respectively). Extractant heptafluoro-dimethyloctanedione (FDOD, 95 %) was obtained from AA Blocks (CA, USA). All reagents employed were of analytical grade and were dissolved in deionized water.

For the measurement of the pH of the aqueous phase, a pH meter (GLP 22, CRISON) was used. For the liquid–liquid extraction process, a thermostatically heated magnetic stirrer (2mag) was employed. A Microwave Plasma-Atomic Emission Spectroscopy (MP-AES 4210, Agilent Technologies) was used to determine concentration of cations in the aqueous solution.

2.2. Experimental procedure

Given the selective extraction of Li^+ from model brines (containing Na^+ , K^+ , Mg^{2+} , Ca^{2+} and Sr^{2+}) with the combinations of extractants DBM•TOPO and FDOD•TOPO previously tested [30], this study goes one step further, with the aim to optimize the conditions of Li^+ separation by considering only this cation in the aqueous phase. Therefore, to prepare this phase, $2.88 \cdot 10^{-4}$ M of Li^+ (2 mg L^{-1} , the maximum concentration found in SWRO concentrates [30]) was dissolved in ultrapure water. A specific volume of NH_3 was added for pH adjustment of the aqueous phase. For the organic phase, TOPO and DBM or FDOD were mixed and diluted in kerosene at different concentrations and molar ratios (see Table 1 for specifications). The mixture was heated at 70°C and shaken on a stirring plate until fully dissolved. Finally, it cooled to room temperature. Both phases were mixed in glass bottles in the same volume ratio ($\text{O/A} = 1$) and stirred at a speed of 500 rpm for 10 min at room temperature. After phase separation, the Li^+ content of the aqueous phase was diluted with ultrapure water and acidified with 5 % HNO_3 , for subsequent measurement by MP-AES. Fig. 1 shows a schematic diagram of the experimental procedure.

The lithium extraction was defined as Eq. (1).

$$\text{Extraction (\%)} = \frac{C_0 - C_e}{C_0} \cdot 100 \quad (1)$$

Table 1
Levels of factors in the CCD of DBM•TOPO and FDOD•TOPO combinations.

| | Factors | Code | Levels | | | | |
|-----------|------------------------------|------|-----------|--------|--------|--------|-----------|
| | | | $-\alpha$ | -1 | 0 | $+1$ | $+\alpha$ |
| DBM•TOPO | [Ext]/[Li ⁺] (-) | A | 48.87 | 100.00 | 175.00 | 250.00 | 301.13 |
| | [NH ₃] (M) | B | 0.26 | 0.60 | 1.10 | 1.60 | 1.94 |
| | X _{DBM} (-) | C | 0.33 | 0.40 | 0.50 | 0.60 | 0.67 |
| FDOD•TOPO | [Ext]/[Li ⁺] (-) | D | 15.91 | 50.00 | 100.00 | 150.00 | 184.09 |
| | pH (-) | E | 9.16 | 9.50 | 10.00 | 10.50 | 10.84 |
| | X _{FDOD} (-) | F | 0.096 | 0.26 | 0.50 | 0.74 | 0.904 |

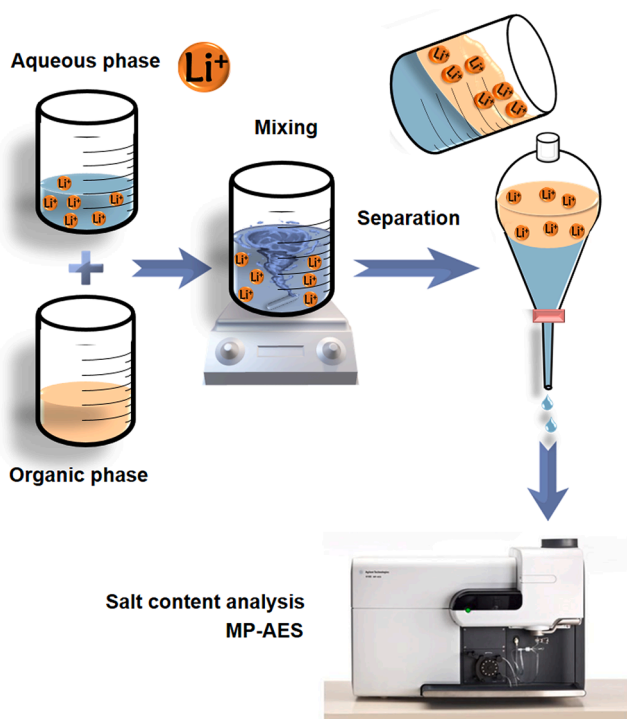


Fig. 1. Schematic illustration of the experimental procedure.

Where C_0 is the initial concentration of Li⁺ (mg L⁻¹), and C_e is the equilibrium concentration of Li⁺ (mg L⁻¹), both in the aqueous phase.

2.3. Experimental design

RSM in combination with statistical analysis (five-level CCD) was applied in order to describe the effects of the selected variables on the lithium extraction efficiency. For each system, the experimental design consisted of three factors (k) of order 3. The variables were coded according to the ranges (levels) of values shown in Table 1 ($-\alpha$ indicates low axial level; -1 low level; 0 the intermediate level; 1 high level; $+\alpha$ high axial level of each factor). The axial points ($-\alpha$ and $+\alpha$) were calculated by the software from a distance of $\alpha = 1.682$ from center, making the design rotatable. The design of the experimental runs, the statistical analyses and the response and contour surfaces were carried out using Minitab 20.4.0.0 software.

For DBM•TOPO system, the independent experimental variables [Ext]/[Li⁺] ratio (A), molar concentration of NH₃ (B) and mole fraction of DBM in the DBM•TOPO mixture (C) were selected. Based on the results obtained experimentally in the previous work, $2.88 \cdot 10^{-4}$ M of Li⁺, pH ≥ 12 and 0.06 M of DBM•TOPO (ratio 1:1) [30], corresponding to a [Ext]/[Li⁺] ≈ 200 , factor A values were selected from 48.87 (0.014 M) to 301.13 (0.087 M). Due to very basic pH values were required to obtain the highest lithium extraction, to simplify laboratory work and to have levels with reasonable spacing between them, and thereby

facilitate calculating, as coded variable B, the NH₃ concentration was used, which varies between a minimum pH of 11.89 (0.26 M) and a maximum of 12.5 (1.94 M). Finally, the mole fraction of DBM, i.e. the ratio DBM/TOPO was studied. This variable had not been experimentally evaluated, however, the literature shows studies that use different solvent ratios as organic phase in order to reach the extraction maximum of the solutes [37–41].

Similarly, for the FDOD•TOPO system design, the independent variables were [Ext]/[Li⁺], pH and mole fraction of FDOD, assigned as D, E and F. The values for the levels were established based on experimental results of the preceding study ($2.88 \cdot 10^{-4}$ M of Li⁺, 0.014 M of FDOD•TOPO (ratio 1:1) and pH ≥ 10 , [30]); thus, ratios from 15.91 (0.005 M) to 184.09 (0.053 M) were used for factor D, pH values between 9.16 and 10.84 for factor E, and a range of factor F from 0.096 to 0.904.

The experimental design points consist of 2^k factorial points with $2k$ axial points and N_c central points (six replicates of the center points) [33], resulting in twenty runs as a complete set of experimental design. The center points were used to determine the experimental error and the reproducibility of the data. Each experimental run was conducted in duplicate to assure the reproducibility. The experimental sequence was randomized to minimize the effects of the uncontrolled factors. The objective function was lithium extraction (Y). A quadratic equation model able to predict the objective function as an approximation of the mathematical relation between the independent variables was employed:

$$Y = \beta_0 + \sum_{i=1}^k \beta_i X_i + \sum_{i=1}^k \beta_{ii} X_i^2 + \sum_{i < j}^{k-1} \beta_{ij} X_i X_j \quad (2)$$

Where Y is the value of the predicted response (lithium extraction percentage), X_i and X_j are the coded values of the independent factors (A, B, C for DBM•TOPO system and D, E, F for FDOD•TOPO system) and β_0 , β_i , β_{ii} and β_{ij} are the model coefficients. The combined effects of variables were evaluated by an analysis of the variance (ANOVA). The quality of the fit polynomial model was dominated by the coefficient of determination of R^2 , and its statistical significance was checked by the F-test in the same program. Model terms were evaluated by the P-value (probability) with 95.0 % confidence level.

3. Results and discussion

In a first stage, quadratic model expressions that describe lithium extraction were obtained for each combination of extractants as a function of the selected variables (factors) using CCD. In a second stage, these equations were used to obtain the response surfaces that predict the behavior of the extraction process and the influence of each variable. Finally, the optimal values that predict the best lithium extraction percentages were determined and experimentally tested.

3.1. Central composite design for lithium extraction

3.1.1. CCD for Li⁺•DBM•TOPO system

The CCD matrix of experiments, their experimental results and the observed response values (predicted from the model) are enumerated in

Table 2

Experimental coded values of the CCD and responses of the DBM•TOPO extractants system.

| Runs | Levels of variable factors (coded) | | | Li ⁺ extraction Response (%) | |
|------|------------------------------------|---------------------------|-------------------------|---|-----------|
| | [Ext]/[Li ⁺] (A) | [NH ₃] (B) | X _{DBM} (C) | Experimental ± error | Predicted |
| 1 | +α | 0 | 0 | 90.87 ± 0.68 | 91.77 |
| 2 | 0 | 0 | +α | 84.13 ± 0.68 | 81.77 |
| 3 | 1 | -1 | 1 | 87.64 ± 0.00 | 89.12 |
| 4 | 0 | 0 | -α | 87.02 ± 0.68 | 92.62 |
| 5 | -1 | -1 | 1 | 57.30 ± 0.00 | 56.09 |
| 6 | 0 | 0 | 0 | 87.98 ± 0.68 | 91.73 |
| 7 | -1 | 1 | 1 | 62.64 ± 0.81 | 64.30 |
| 8 | 0 | 0 | 0 | 87.98 ± 0.68 | 91.73 |
| 9 | -1 | -1 | -1 | 70.22 ± 0.79 | 68.12 |
| 10 | 1 | -1 | -1 | 95.51 ± 0.00 | 89.99 |
| 11 | 0 | 0 | 0 | 94.23 ± 0.00 | 91.73 |
| 12 | 0 | 0 | 0 | 93.75 ± 0.68 | 91.73 |
| 13 | 0 | +α | 0 | 92.86 ± 0.00 | 92.83 |
| 14 | 0 | -α | 0 | 75.77 ± 0.73 | 79.04 |
| 15 | 0 | 0 | 0 | 93.27 ± 0.00 | 91.73 |
| 16 | -α | 0 | 0 | 43.27 ± 2.72 | 45.61 |
| 17 | 1 | 1 | 1 | 97.13 ± 0.81 | 97.32 |
| 18 | 1 | 1 | -1 | 97.70 ± 0.00 | 98.19 |
| 19 | 0 | 0 | 0 | 93.75 ± 0.68 | 91.73 |
| 20 | -1 | 1 | -1 | 80.46 ± 0.00 | 76.32 |

Table 2. The Pareto chart (Fig. 2a) shows that both the [Ext]/[Li⁺] and [NH₃] variables have a positive influence on lithium extraction; increasing these variables results in an increase in extraction percentages. The molar ratio [Ext]/[Li⁺] presents the greatest influence. On the other hand, the X_{DBM} fraction shows a significant but negative influence.

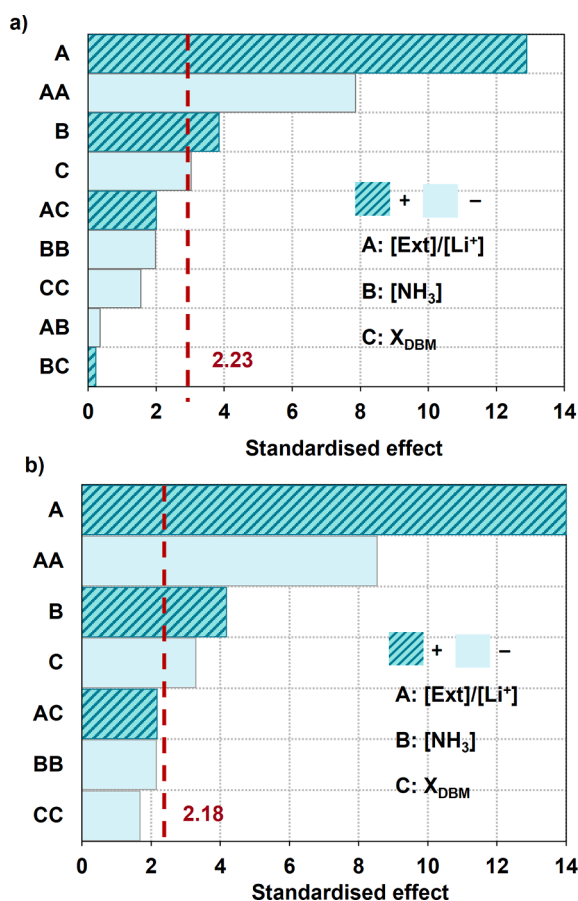


Fig. 2. Pareto chart of effects showing the significance of the linear and quadratic effects for the DBM•TOPO system a) all the standardized effects and b) excluding BC and AB interactions.

Table 3

Analysis of Variance (ANOVA) for Li⁺ extraction using DBM•TOPO extractant combination.

| Model terms | Sum of Squares (SS) | Degree of Freedom (DF) | Mean Square (MS) | F-Value | P-value | Remarks |
|-------------------------|---------------------|------------------------|------------------|---------|---------|-------------|
| A* | 2571.20 | 1 | 2571.20 | 196.02 | 0.0000 | Significant |
| B* | 229.54 | 1 | 229.54 | 17.50 | 0.0013 | Significant |
| C* | 141.95 | 1 | 141.95 | 10.82 | 0.0065 | Significant |
| AA | 956.90 | 1 | 956.90 | 72.95 | 0.0000 | Significant |
| AC | 62.15 | 1 | 62.15 | 4.74 | 0.0464 | Significant |
| BB | 60.60 | 1 | 60.60 | 4.62 | 0.0483 | Significant |
| CC | 37.10 | 1 | 37.10 | 2.83 | 0.1184 | |
| Lack of fit | 112.56 | 7 | 16.08 | 1.79 | 0.2695 | |
| Pure error | 44.84 | 5 | 8.97 | | | |
| Cor total | 4148.43 | 19 | | | | |
| R ² | 96.21 | | | | | |
| Adjusted R ² | 93.99 | | | | | |

* A: [Ext]/[Li⁺]; B: [NH₃]; C: X_{DBM}.

The quadratic effect of [Ext]/[Li⁺] (AA in the chart) also becomes statistically significant. The interactions between [Ext]/[Li⁺] and [NH₃] (AB) and that between [NH₃] and X_{DBM} (BC) were the smallest effects and did not exceed the significance limit, i.e. interactions that may occur between these sets of variables do not influence Li⁺ extraction. Therefore, for a correct and simplified analysis, these variables were excluded, resulting in a new Pareto chart (Fig. 2b), in which, finally the main effects are found.

The main statistical parameters obtained from the analysis of variance (ANOVA) are listed in Table 3. The simplified regression equation obtained from the analysis and based on the significant model terms are shown (in their coded form) in Eq. (3).

$$\text{Extraction (\%)} = 4.90 + 0.50 \cdot A + 26.24 \cdot B + 63.0 \cdot C - 0.0015 \cdot A^2 + 0.37 \cdot AC - 8.20 \cdot B^2 - 160.40 \cdot C^2 \quad (3)$$

As shown in Table 3, the adjusted determination coefficient of R² was higher than 90, indicating the accuracy of the model to describe the experimental data adequately [42]. This result has been obtained excluding the least significant interactions, AB and BC. The complete ANOVA table with all the resulting interactions can be found in the supplementary material (Table S.1). The lack-of-fit test is designed to determine whether the selected model is adequate to describe the observed data or whether a more complicated model should be used. Since the P-value for the lack of fit in the ANOVA table is >0.05 (0.27), the model appears to be adequate for the observed data at the 95.0% confidence level, validating the significance of this model.

Fig. 3 shows the more relevant statistical plots that complement the study of the regression model fit for lithium extraction with the DBM•TOPO combination. Fig. 3a illustrates the plot of residuals versus predicted residuals. The random distribution of the points confirms the adequacy of the proposed model and proves the constant variance hypothesis. Fig. 3b shows the normal probability (%) versus the residuals. The normal distribution approaching a straight line indicates the accuracy of the model, as residuals that approach a straight line and distribute the errors uniformly support the adequacy of the least squares fit. Fig. 3c shows the experimentally observed responses versus the values predicted by the model. It can be observed that all design points were scattered along and very close to the diagonal line. This indicates that the responses of the experimental results were well adjusted in the range of variance compared to the predicted values determined from the respective empirical models [33].

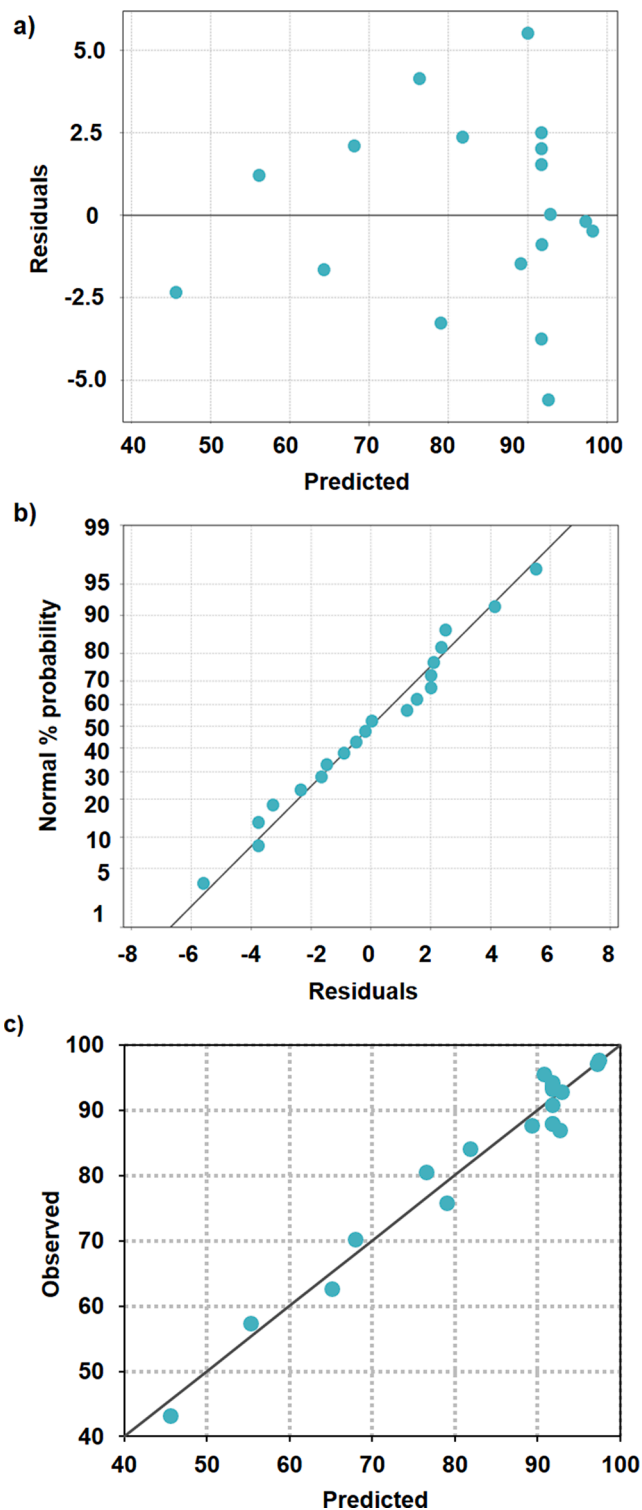


Fig. 3. Statistical results of the CCD for Li^+ extraction using DBM•TOPO extractant system of (a) Residual vs predicted response; (b) Normal probability of residuals; (c) Observed vs predicted values.

3.1.2. CCD for Li^+ •FDOD•TOPO system

In the FDOD•TOPO extractants system, the three operating variables that influence the Li^+ extraction efficiency, extractant to lithium concentration ratio, initial pH and FDOD molar ratio, have been optimized based on CCD. The CCD matrix of experiments and the observed response values are enumerated in Table 4. The Pareto chart for this system (Fig. 4a) shows that the most statistically significant variable for

Table 4

Experimental coded values of the CCD and responses of the FDOD•TOPO extractants system.

| Runs | Levels of variable factors (coded) | | | Li^+ extraction (%) Response | | |
|------|------------------------------------|------------|-----------------------|---------------------------------------|------------------|--------|
| | [Ext]/[Li^+] (D) | pH (E) | X_{FDOD} (F) | Experimental \pm error | Predicted | |
| 1 | -1 | 1 | 1 | -1 | 87.50 \pm 0.00 | 103.52 |
| 2 | 1 | -1 | -1 | 1 | 0.00 \pm 1.54 | -11.71 |
| 3 | -1 | -1 | -1 | -1 | 0.00 \pm 0.77 | -0.23 |
| 4 | 1 | 1 | 1 | -1 | 97.40 \pm 0.74 | 94.90 |
| 5 | 0 | 0 | 0 | 0 | 53.54 \pm 1.43 | 44.84 |
| 6 | 0 | 0 | 0 | - α | 93.94 \pm 0.00 | 79.89 |
| 7 | 0 | 0 | 0 | 0 | 52.53 \pm 0.00 | 44.84 |
| 8 | -1 | -1 | 1 | 1 | 0.00 \pm 0.00 | 6.80 |
| 9 | - α | 0 | 0 | 0 | 26.26 \pm 1.43 | 21.49 |
| 10 | 0 | 0 | 0 | 0 | 45.96 \pm 2.14 | 44.84 |
| 11 | 0 | - α | 0 | 0 | 0.00 \pm 2.26 | -5.60 |
| 12 | 1 | -1 | -1 | -1 | 0.00 \pm 0.00 | 15.38 |
| 13 | 0 | 0 | 0 | + α | 0.00 \pm 1.43 | 9.80 |
| 14 | 0 | 0 | 0 | 0 | 41.41 \pm 1.43 | 44.84 |
| 15 | + α | 0 | 0 | 0 | 0.00 \pm 2.14 | -1.32 |
| 16 | -1 | 1 | 1 | 1 | 58.33 \pm 0.00 | 47.26 |
| 17 | 0 | + α | 0 | 0 | 98.96 \pm 0.00 | 95.29 |
| 18 | 1 | 1 | 1 | 1 | 0.00 \pm 0.00 | 4.53 |
| 19 | 0 | 0 | 0 | 0 | 38.38 \pm 1.43 | 44.84 |
| 20 | 0 | 0 | 0 | 0 | 34.85 \pm 0.71 | 44.84 |

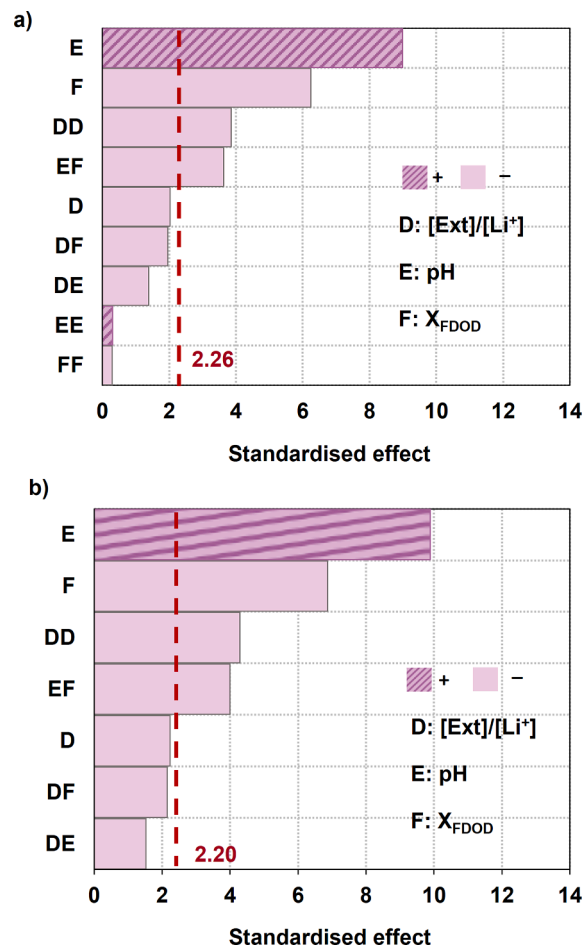


Fig. 4. Pareto chart of effects showing the significance of the linear and quadratic effects for the FDOD•TOPO system a) all the standardized effects and b) excluding EE and FF interactions.

Table 5
Analysis of Variance (ANOVA) for Li⁺ extraction using FDOD•TOPO extractant combination.

| Model terms | Sum of Squares (SS) | Degree of Freedom (DF) | Mean Square (MS) | F-Value | P-value | Remarks |
|-------------------------|---------------------|------------------------|------------------|---------|---------|-------------|
| D* | 627.79 | 1 | 627.79 | 4.99 | 0.0471 | Significant |
| E* | 12288.44 | 1 | 12288.44 | 97.76 | 0.0000 | Significant |
| F* | 5929.11 | 1 | 5929.11 | 47.17 | 0.0000 | Significant |
| DD | 2311.26 | 1 | 2311.26 | 18.39 | 0.0013 | Significant |
| DE | 293.18 | 1 | 293.18 | 2.33 | 0.1549 | |
| DF | 581.92 | 1 | 581.92 | 4.63 | 0.0545 | |
| EF | 2002.50 | 1 | 2002.50 | 15.93 | 0.0021 | Significant |
| Lack of fit | 1189.59 | 5 | 169.94 | 3.16 | 0.1137 | |
| Pure error | 288.44 | 5 | 57.69 | | | |
| Cor total | 25416.96 | 19 | | | | |
| R ² | 94.18 | | | | | |
| Adjusted R ² | 90.79 | | | | | |

* D: [Ext]/[Li⁺]; E: pH; F: X_{FDOD}.

lithium extraction, with a positive trend, is pH. After that, the fraction X_{FDOD} is the second most influential variable on the extraction, but in this case, it is negative; an increase in X_{FDOD} would give lower results of lithium extraction. The quadratic effect of [Ext]/[Li⁺] also has a negative effect, but it is not very far from the limit, so its effect does not have much relevance. The quadratic effects of pH (EE) and mole fraction (FF) are the least statistically significant, so it was decided to exclude them in the final analysis. Eliminating these variables, the final Pareto plot is shown in Fig. 4b.

The main statistical parameters obtained from the Analysis of variance (ANOVA) are listed in Table 5. As shown in that table, the adjusted determination coefficient of R² was 90.79 %, excluding the less significant interactions (EE and FF). The complete ANOVA table with all the resulting interactions can be found in the Supplementary material (Table S.2). This result shows the adequacy of the model to describe the experimental data. This model also exceeds the lack-of-fit test with a value > 0.05 (excluding EE and FF interactions increases to 0.11), validating the significance of the model with a 95.0 % confidence level. The simplified regression equation obtained from the analysis and based on the significant model terms are shown (in their coded form) in Eq. (4).

$$\begin{aligned} \text{Extraction (\%)} = & -1484.18 + 3.62 \cdot D + 150.13 \cdot E + 1302.69 \cdot F - 0.0049 \cdot D^2 \\ & - 0.24 \cdot DE - 0.71 \cdot DF - 131.84 \cdot EF \end{aligned} \quad (4)$$

Fig. 5 shows statistical plots that complement the study of the regression model fit for lithium extraction with the FDOD•TOPO combination, as was done with the previous combination. The random distribution of the points in Fig. 5a proves the constant variance hypothesis, supporting the adequacy of the proposed model. The normal distribution of the points nearing a straight line in Fig. 5b indicates the accuracy of the model. It can be observed in Fig. 5c that all the design points were scattered along the diagonal line, some closer and some further apart. This is because the calculated model has a large number of coefficients and these coefficients are likely to have high confidence intervals. As a result, when trying to make predictions with the equation, high confidence intervals are obtained.

3.2. Response surface methodology

Expressions (3) and (4), obtained in Sections 3.1.1 and 3.1.2, have been used to create three-dimensional (3D) response surfaces and contour plots with the aim to visualize how the variables behave with each other and how they affect the response. The surfaces are plotted with

two variables on the abscissa and the % Li⁺ extraction obtained on the ordinates, keeping fixed the third variable at its central level value (0), as is characteristic of this type of analysis.

3.2.1. RSM for Li⁺•DBM•TOPO system

Fig. 6 shows the response surfaces obtained when plotting Eq. (3). In these plots, curvatures indicate possible interactions between the factors. The graphical representation of the model equation allows, on the one hand, a more intuitive and visual prediction of the effect of each variable in the system, and on the other hand, to determine the values of the factors able to optimize Li⁺ extraction. In Fig. 6a, it can be observed that the Li⁺ extraction response can change drastically depending on the values of the independent variables. With a fixed value of X_{DBM} = 0.5, the increase in [Ext]/[Li⁺] is very significant (black line, 3D Figure), while an increase in [NH₃] has a smaller effect. For a [Ext]/[Li⁺] = 50, with low [NH₃] (0.26 M) extractions of 33 % are achieved, and for high [NH₃] (1.94 M) it reaches 47 %, low values for the desired level of lithium separation. The maximum predicted extraction is 99.53 %, with [Ext]/[Li⁺] = 233.55 and a [NH₃] = 1.59 M (dashed black lines, 2D Figure). In Fig. 6b, the interaction of [NH₃] and X_{DBM} appears to be weak when [Ext]/[Li⁺] is fixed at 175, as evidenced by the response surface having low slopes. The minimum extraction is 60.5 % when X_{DBM} = 0.70 and [NH₃] = 0.1 M, while the maximum extraction, 95.4 %, is predicted for X_{DBM} = 0.40 and [NH₃] = 1.58 (black lines, 2D Figure). In Fig. 6c, with a fixed [NH₃] = 1.1 M (pH of 12.12), low Li⁺ extraction percentages (below 20 %) are obtained at low [Ext]/[Li⁺] ratios (from 0 to 30), particularly for high values of X_{DBM} (from 0.5 to 0.7) (pink line, 3D Figure). However, from a [Ext]/[Li⁺] ratio of 200–260, higher lithium extraction results are obtained, around 90 %, over the whole studied ratio X_{DBM}, from 0.3 to 0.7 (black lines 3D and 2D Figures).

3.2.2. RSM for Li⁺•FDOD•TOPO system

Similar to section 3.2.1., in Fig. 7 3D response surfaces and contour plots of the FDOD•TOPO extractant system are shown. Fig. 7a demonstrates that, with a fixed value of X_{FDOD} = 0.5, increasing the [Ext]/[Li⁺] ratio does not necessarily result in an increased response (black line, 3D Figure), but instead, the effect of pH is more pronounced (pink line, 3D Figure). Li⁺ extraction does not occur for a pH lower than 9.50, regardless of the [Ext]/[Li⁺] ratio. However, it is possible to reach 100 % Li⁺ extraction at pH close to 11 and [Ext]/[Li⁺] ratios between 25 and 100 (dashed lines, 2D Figure). Fig. 7b shows that for [Ext]/[Li⁺] = 100, higher Li⁺ extraction is predicted using the highest pH, 11, and the lowest X_{FDOD} values, 0 (intersection between black and pink lines, 3D Figure), which means, that even with a small amount of the

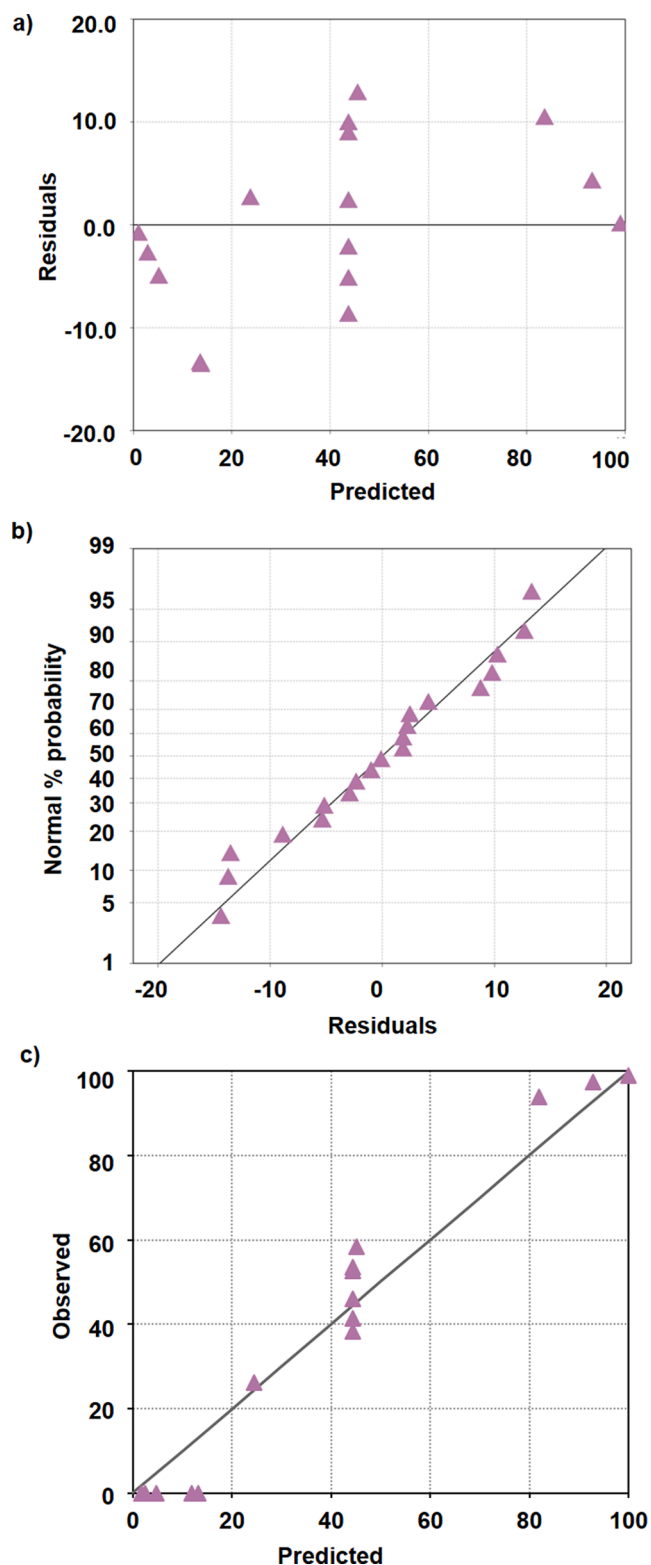


Fig. 5. Statistical results of the CCD for Li^+ extraction using FDOD•TOPO extractant system of (a) Residual vs predicted response; (b) Normal probability of residuals; (c) Observed vs predicted values.

β -diketone FDOD, in synergy with the organophosphate TOPO, high lithium extractions can be achieved. The optimal conditions for achieving maximum extraction (100 %) are an X_{FDOD} value of 0.26, and a pH of 10.38 (dashed lines, 2D Figure), which means that an amount of TOPO can be replaced by the effect of fluorine atoms from FDOD during to the Li^+ extraction process [24]. Finally, Fig. 7c indicates that when the initial pH is set to 10, the predicted lithium extraction responses are low across all ranges of the other two independent variables studied, especially for high X_{FDOD} values (black line, 3D Figure). Maximum extraction of 90 % can be achieved at $X_{\text{FDOD}}=0$ and $[\text{Ext}]/[\text{Li}^+] = 112.5$, but working to initial pH value, 10, which is not the most favorable for the system. As it has been possible to verify through this analysis, the obtained regression models can be used to optimize the conditions of lithium extraction using the combination of these β -diketones and TOPO as extractant.

3.3. Lithium optimum separation using the predictive models

Once the models that describe the influence of each factor on Li^+ extraction were obtained using the optimization function of the Minitab software, the optimum values of each factor leading to maximum extraction were determined. For the Li^+ •DBM•TOPO system, the optimal values were $[\text{Ext}]/[\text{Li}^+]$ ratio of 232.33 (corresponding to an extractant concentration of 0.067 M), NH_3 concentration of 1.6 M (equivalent to an initial pH value of 12.46) and X_{DBM} of 0.46. Table 6 shows the predicted Li^+ extraction percentage under these conditions and the experimentally obtained results, being 99.70 % and 96.97 % respectively, falling within the confidence interval of the model (95 %). In comparison with the obtained previous results [30] shown in Table 6 (previous studies column), there are only minor differences. A slightly higher pH value, from 12.2 to 12.46, and less than 0.5 X_{DBM} , which is lower than the 1:1 ratio used in the initial results, 0.46, in order to obtain a Li^+ extraction too slightly higher, from 95.4 % to around 97 %.

For the Li^+ •FDOD•TOPO system, the optimal values of the factors have been calculated with the desired objective of achieving a response of 100 %, resulting in the optimal conditions of $[\text{Ext}]/[\text{Li}^+]$ ratio of 92.61 (0.027 M of extractant), initial pH of 10.38 and a X_{FDOD} of 0.26. It is worthy to mention that commercial FDOD is 58 times more expensive than DBM, while TOPO is currently quite an affordable chemical [43–45]. In this sense, the results of this study economically boost the maturity of the process through the minimization of the reagent that is used with TOPO. The predicted Li^+ extraction with these conditions and that obtained experimentally are presented in Table 6, being 100 % and 97.03 % respectively, falling within the confidence interval of the model (95 %). The optimization results, in this case, differ more from the obtained values in a previous study. A higher amount of extractant is required, from 0.014 to 0.027 M. The required pH has been successfully reduced to 10.38. Although it is still necessary to vary the pH further, as these concentrates typically have a pH ranging between 8 and 8.5 [46], the significant reduction in the pH adjustment required is an encouraging result. Notably, the FDOD:TOPO ratio is crucial, as a FDOD fraction of 0.26 is optimal for the process versus the ratio 1:1 from previous results. The Li^+ extraction is similar, from 98.7 % in previous studies to 97.0 %, but reducing the consumption of this β -diketone is a key experimental factor as its market price is higher than that of TOPO.

The obtained results from both systems validate the reliability and accuracy of the prediction and optimization models, thus the predicted results were experimentally validated and found to be within the expected range, consistent with previous studies.

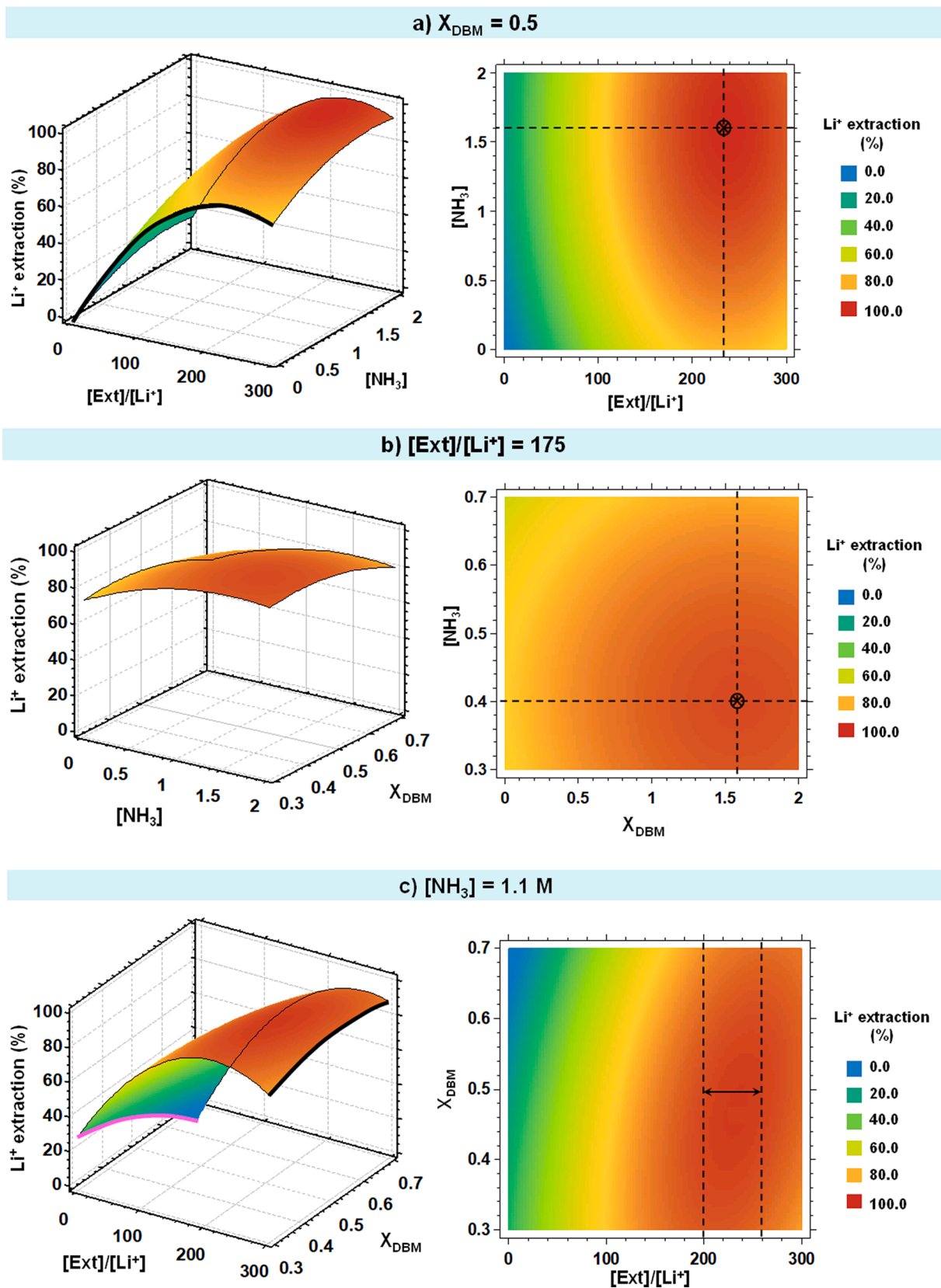


Fig. 6. Response surface and contour plots for Li^+ extraction with the fixed conditions (a) $X_{DBM} = 0.5$; (b) $[Ext]/[Li^+] = 175$; (c) $[NH_3] = 1.1$ M.

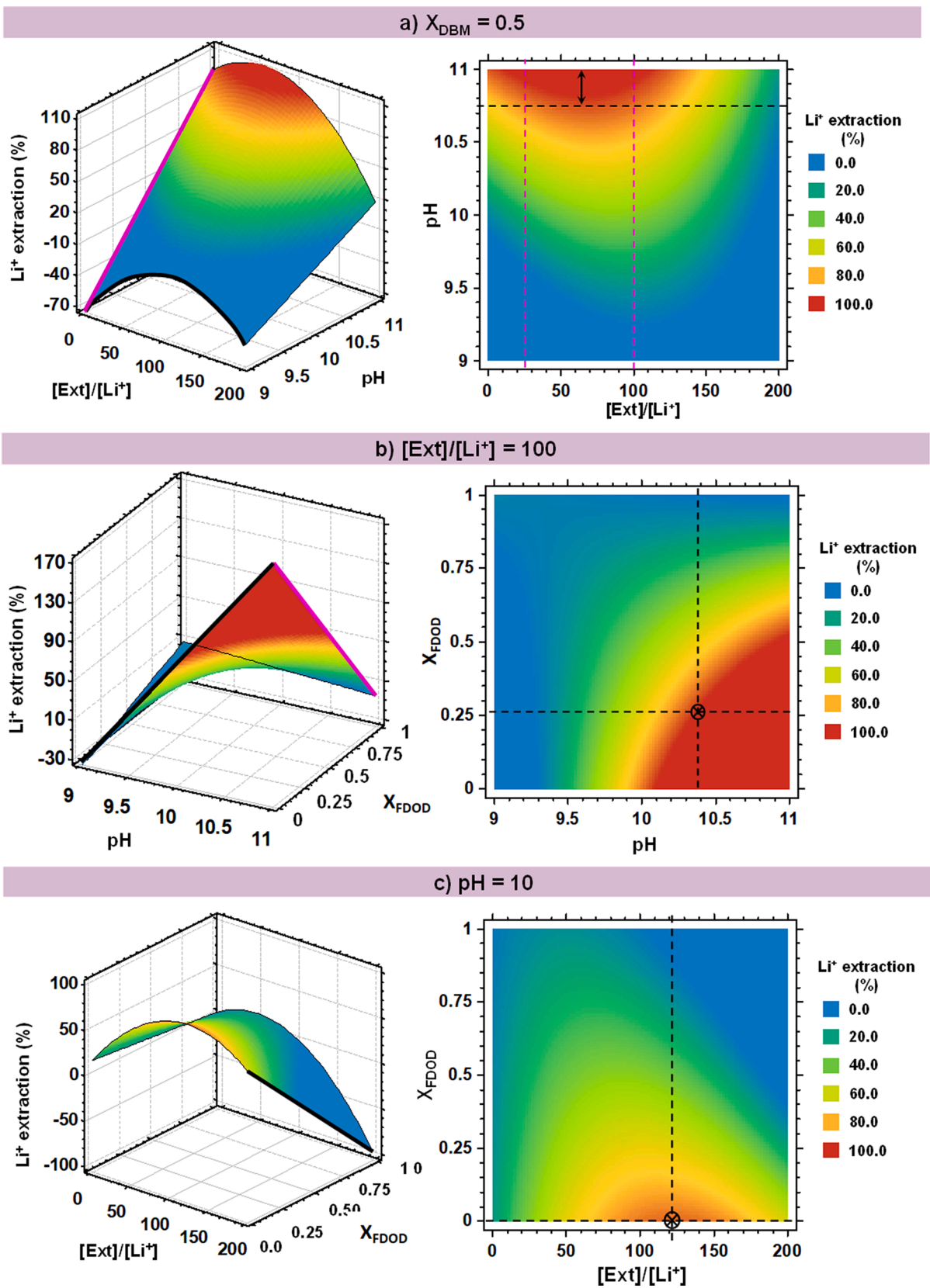


Fig. 7. Response surface and contour plots for Li⁺ extraction with the fixed conditions (a) $X_{FDOD} = 0.5$; (b) $[Ext]/[Li^+] = 100$; (c) $pH = 10$.

Table 6

Predicted and experimental responses of Li⁺ extraction for validation of CCD designs using DBM•TOPO and FDOD•TOPO. Comparison with results obtained in previous studies.

| | DBM•TOPO | | FDOD•TOPO | |
|--------------------------------------|-----------------------|-----------------------------|-----------------------|-----------------------------|
| | Previous studies [30] | Optimal conditions obtained | Previous studies [30] | Optimal conditions obtained |
| [Extractant] [M] | ≥ 0.06 | 0.07 | ≥ 0.014 | 0.027 |
| Initial pH | > 12.00 | 12.46 | > 11.00 | 10.38 |
| X _{β-diketone} | = 0.50 | 0.46 | = 0.50 | 0.26 |
| Li ⁺ extraction rate (%)* | | 99.70 | | 100.00 |
| Li ⁺ extracted (%)** | 95.40 | 97.00 | 98.70 | 97.00 |
| 95 % confidence interval | | 95.65–103.75 | | 94.42–105.58 |

*RSM predicted value**Experimental value.

4. Conclusions

In this study, the optimal operation conditions which lead to maximum separation of lithium employing the extractant combinations DBM•TOPO and FDOD•TOPO have been evaluated in low concentrations (2 mg L⁻¹) ideal solutions. The study successfully used response surface methodology (RSM) to analyze the effect of each operation variable on lithium separation for both systems, as well as to predict the maximum lithium extraction rate for a given operating conditions (extractant concentration, basicity of the aqueous phase and molar ratio between extractants).

For DBM•TOPO system, the variables [Ext]/[Li⁺] and [NH₃] presented the most positive effects on extraction. The optimal extraction conditions for the DBM•TOPO system were a [Ext]/[Li⁺] ratio of 232.33 (0.067 M), a NH₃ concentration of 1.60 M (pH of 12.46), and a X_{DBM} of 0.46, yielding a Li⁺ extraction rate of 96.97 % (R² = 93.99).

In the case of FDOD•TOPO, pH showed the greatest positive effect on the extraction, followed by X_{FDOD} (with negative effect). The optimal conditions reached were, a [Ext]/[Li⁺] ratio of 92.61 (0.027 M), a pH value of 10.38 and a X_{FDOD} of 0.26, which lead to obtaining Li⁺ extraction rate of 97.03 % (R² = 90.79).

Comparing the predicted model results using RSM with the previous experimental results for both systems, it is required an extractant concentration in the order of 10⁻², whereas a higher amount of TOPO than β-diketone is required (β-diketone:TOPO < 1). The reduction of the β-diketone:TOPO ratio is significant due to the higher price of β-diketones, particularly FDOD, so that allows for a reduction in the ratio while achieving practically the same Li⁺ extraction value, favoring the economy of the process.

In conclusion, this study presents an innovative and viable system for extracting lithium from desalination concentrates. The application of statistical analysis has proven to be a valuable tool, enabling the reduction of the number of experiments required in the extraction systems. This approach not only enhances the efficiency of the process but also contributes to the overall feasibility and practicality of the lithium recovery method proposed in this research.

CRedit authorship contribution statement

E. Fernández-Escalante: Investigation, Conceptualization, Methodology, Writing – review & editing. **R. Ibañez:** Investigation, Conceptualization, Methodology, Writing – review & editing, Funding acquisition. **Ma.-F. San-Román:** Investigation, Conceptualization, Methodology, Formal analysis, Writing – review & editing, Supervision, Funding acquisition.

Declaration of Competing Interest

The authors declare that they have no known competing financial interests or personal relationships that could have appeared to influence the work reported in this paper.

Acknowledgments

This research was developed in the framework of the projects PID2020-115409RB-I00, PDC2021-120786-I00 and TED2021-129874B-I00 financed by the Ministry of Science and Innovation (Spain). Elena Fernández-Escalante is grateful for the predoctoral contract PRE2021-100160.

Appendix A. Supplementary material

Supplementary data to this article can be found online at <https://doi.org/10.1016/j.seppur.2023.124645>.

References

- [1] M. Date, V. Patyal, D. Jaspal, A. Malviya, K. Khare, Zero liquid discharge technology for recovery, reuse, and reclamation of wastewater: A critical review, *J. Water Process Eng.* 49 (2022), <https://doi.org/10.1016/j.jwpe.2022.103129>.
- [2] European Commission, COM 98 final, 2020. <https://www.un.org/sustainabledevelopment/sustainable-consumption-production/> (accessed January 18, 2023).
- [3] R. Molinari, A.H. Avci, P. Argurio, E. Curcio, S. Meca, M. Plà-Castellana, J. L. Cortina, Selective precipitation of calcium ion from seawater desalination reverse osmosis brine, *J. Clean. Prod.* 328 (2021), <https://doi.org/10.1016/j.jclepro.2021.129645>.
- [4] K. Elsaid, E.T. Sayed, M.A. Abdelkareem, A. Baroutaji, A.G. Olabi, Environmental impact of desalination processes: Mitigation and control strategies, *Sci. Total Environ.* 740 (2020), <https://doi.org/10.1016/j.scitotenv.2020.140125>.
- [5] J.L. Mero, *The mineral resources of the sea*, Elsevier, Amsterdam, 1965.
- [6] R.S. Al-Absi, M.H. Abu-Dieyeh, R. Ben-Hamadou, M.S. Nasser, M.A. Al-Ghouti, Thermodynamics, isotherms, and mechanisms studies of lithium recovery from seawater desalination reverse osmosis brine using roasted and ferrocyanide modified date pits, *Environ. Technol. Innov.* 25 (2022), <https://doi.org/10.1016/j.eti.2021.102148>.
- [7] P. Loganathan, G. Naidu, S. Vigneswaran, Mining valuable minerals from seawater: A critical review, *Environ. Sci. (Camb.)* 3 (2017) 37–53, <https://doi.org/10.1039/c6ew00268d>.
- [8] M. Palmeros Parada, P. Kehrein, D. Xevgenos, L. Asveld, P. Osseweijer, Societal values, tensions and uncertainties in resource recovery from wastewaters, *J. Environ. Manage.* 319 (2022), <https://doi.org/10.1016/j.jenvman.2022.115759>.
- [9] X. Zhang, W. Zhao, Y. Zhang, V. Jegatheesan, A review of resource recovery from seawater desalination brine, *Rev. Environ. Sci. Biotechnol.* 20 (2021) 333–361, <https://doi.org/10.1007/s11157-021-09570-4>.
- [10] I. Ihsanullah, J. Mustafa, A.M. Zafar, M. Obaid, M.A. Atieh, N. Ghaffour, Waste to wealth: A critical analysis of resource recovery from desalination brine, *Desalination* 543 (2022), <https://doi.org/10.1016/j.desal.2022.116093>.
- [11] U. Bardi, Extracting minerals from seawater: An energy analysis, *Sustainability* 2 (2010) 980–992, <https://doi.org/10.3390/su2040980>.
- [12] A. Shahmansouri, J. Min, L. Jin, C. Bellona, Feasibility of extracting valuable minerals from desalination concentrate: A comprehensive literature review, *J. Clean. Prod.* 100 (2015) 4–16, <https://doi.org/10.1016/j.jclepro.2015.03.031>.
- [13] M.A. Hussain, Process for pre-treating and desalinating seawater, Patent No. US7198722 (2007), U.S. Patent and Trademark Office.
- [14] A. Arakel, H. Tian, L.J. Stapleton, Process for the treatment of saline water, Patent No. US7595001B2 (2009), U.S. Patent and Trademark Office.
- [15] A. Buenaventura Pouyfaucou, Brine treatment process, Patent No. ES2390166A1 (2012), Spanish Patent and Trademark Office.
- [16] D. Fontana, F. Forte, M. Pietrantonio, S. Pucciarmati, C. Marcoaldi, Magnesium recovery from seawater desalination brines: a technical review, *Environ. Dev. Sustain.* (2022), <https://doi.org/10.1007/s10668-022-02663-2>.

- [17] M. Ahmad, B. Garudachari, Y. Al-Wazzan, R. Kumar, J.P. Thomas, Mineral extraction from seawater reverse osmosis brine of gulf seawater, *Desalination, Water Treat.* 144 (2019) 45–56, <https://doi.org/10.5004/dwt.2019.23679>.
- [18] A. Khalil, S. Mohammed, R. Hashaikheh, N. Hilal, Lithium recovery from brine: Recent developments and challenges, *Desalination* 528 (2022), <https://doi.org/10.1016/j.desal.2022.115611>.
- [19] J. Wang, X. Yue, P. Wang, T. Yu, X. Du, X. Hao, A. Abudula, G. Guan, Electrochemical technologies for lithium recovery from liquid resources: A review, *Renew. Sustain. Energy Rev.* 154 (2022), <https://doi.org/10.1016/j.rser.2021.111813>.
- [20] T. Sampedro, C. Tristán, L. Gómez-Coma, J. Rioyo, M. Sainz, I. Ortiz, R. Ibañez, SWRO concentrates for more efficient wastewater reclamation, *Desalination* 545 (2023), <https://doi.org/10.1016/j.desal.2022.116156>.
- [21] Á. Rivero-Falcón, B. Peñate Suárez, N. Melián-Martel, SWRO Brine Characterisation and Critical Analysis of Its Industrial Valorisation: A Case Study in the Canary Islands (Spain), *Water (Switzerland)* 15 (2023), <https://doi.org/10.3390/w15081600>.
- [22] U.S. Geological Survey, MINERAL COMMODITY SUMMARIES 2022, 2022. Doi: Doi:10.3133/mcs2022.
- [23] Y. Zhang, L. Wang, W. Sun, Y. Hu, H. Tang, Membrane technologies for Li+/Mg2+ separation from salt-lake brines and seawater: A comprehensive review, *J. Ind. Eng. Chem.* 81 (2020) 7–23, <https://doi.org/10.1016/j.jiec.2019.09.002>.
- [24] P. Shi, S. Yang, G. Wu, H. Chen, D. Chang, Y. Jie, G. Fang, C. Mo, Y. Chen, Efficient separation and recovery of lithium and manganese from spent lithium-ion batteries powder leaching solution, *Sep. Purif. Technol.* 309 (2023), <https://doi.org/10.1016/j.seppur.2022.123063>.
- [25] U.S. Geological Survey, MINERAL COMMODITY SUMMARIES 2023, 2023. Doi: Doi:10.3133/mcs2023.
- [26] G. Liu, Z. Zhao, A. Ghahreman, Novel approaches for lithium extraction from salt-lake brines: A review, *Hydrometall.* 187 (2019) 81–100, <https://doi.org/10.1016/j.hydromet.2019.05.005>.
- [27] P.K. Choubey, K.S. Chung, M. seuk Kim, J. chun Lee, R.R. Srivastava, Advance review on the exploitation of the prominent energy-storage element Lithium. Part II: From sea water and spent lithium ion batteries (LIBs), *Miner Eng.* 110 (2017) 104–121. Doi:10.1016/j.mineng.2017.04.008.
- [28] B. Swain, Recovery and recycling of lithium: A review, *Sep. Purif. Technol.* 172 (2017) 388–403, <https://doi.org/10.1016/j.seppur.2016.08.031>.
- [29] R. Coterillo, L.E. Gallart, E. Fernández-Escalante, J. Junquera, P. García-Fernández, I. Ortiz, R. Ibañez, M.F. San-Román, Selective extraction of lithium from seawater desalination concentrates: Study of thermodynamic and equilibrium properties using Density Functional Theory (DFT), *Desalination* 532 (2022), <https://doi.org/10.1016/j.desal.2022.115704>.
- [30] E. Fernández-Escalante, R. Ibañez, M.F. San Román, Selective lithium separation from desalination concentrates via synergy of extractants mixtures, *Desalination* 556 (2023), <https://doi.org/10.1016/j.desal.2023.116525>.
- [31] V. Kumar, A. Al-Gheethi, S.M. Asharuddin, N. Othman, Potential of cassava peels as a sustainable coagulant aid for institutional wastewater treatment: Characterisation, optimisation and techno-economic analysis, *Chem. Eng. J.* 420 (2021), <https://doi.org/10.1016/j.cej.2020.127642>.
- [32] R.H. Myers, D.C. Montgomery, C.M. Anderson-Cook, *Response Surface Methodology: Process and Product Optimization Using Designed Experiments*, 4th ed., John Wiley and Sons, Hoboken, New Jersey, 2016.
- [33] George E.P. Box, J. Stuart Hunter, William G. Hunter, *Statistics for Experimenters: Design, Innovation and Discovery*, 2nd Ed., New Jersey, 2005.
- [34] D. Dutta, R. Panda, A. Kumari, S. Goel, M.K. Jha, Sustainable recycling process for metals recovery from used printed circuit boards (PCBs), *Sustain. Mater. Technol.* 17 (2018), <https://doi.org/10.1016/j.susmat.2018.e00066>.
- [35] A.F. Mohammad, M.H. El-Naas, A.H. Al-Marzouqi, M.I. Suleiman, M. Al Musharfy, Optimization of magnesium recovery from reject brine for reuse in desalination post-treatment, *Journal of Water, Process. Eng.* 31 (2019), <https://doi.org/10.1016/j.jwpe.2019.100810>.
- [36] E. Katoozi, Z. Anari, Statistical optimization of extraction column parameters for the zinc (II) solvent extraction by D2EHPA in a continuous mode, *Miner. Eng.* 174 (2021), <https://doi.org/10.1016/j.mineng.2021.107255>.
- [37] Y.-S. Kim, G. In, J.-M. Choi, Chemical Equilibrium and Synergism for Solvent Extraction of Trace Lithium with Thenoyltrifluoroacetone in the Presence of Trioctylphosphine Oxide, 2003.
- [38] G.R. Harvianto, S.G. Jeong, C.S. Ju, The effect of dominant ions on solvent extraction of lithium ion from aqueous solution, *Korean J. Chem. Eng.* 31 (2014) 828–833, <https://doi.org/10.1007/s11814-014-0005-7>.
- [39] L. Zhang, L. Li, D. Shi, X. Peng, F. Song, F. Nie, Kinetics and mechanism study of lithium extraction from alkaline solution by HFTA and TOPO and stripping process using Lewis cell technique, *Sep. Purif. Technol.* 211 (2019) 917–924, <https://doi.org/10.1016/j.seppur.2018.10.043>.
- [40] L. Zhang, L. Li, H. Rui, D. Shi, X. Peng, L. Ji, X. Song, Lithium recovery from effluent of spent lithium battery recycling process using solvent extraction, *J. Hazard. Mater.* 398 (2020), 122840, <https://doi.org/10.1016/j.jhazmat.2020.122840>.
- [41] G. Zante, M. Boltoeva, A. Masmoudi, R. Barillon, D. Trébouet, Highly selective transport of lithium across a supported liquid membrane, *J. Fluor. Chem.* 236 (2020), 109593, <https://doi.org/10.1016/j.jfluchem.2020.109593>.
- [42] R. G.D. Steel, James.H. Torrie, *Principles and Procedures of Statistics with Special Reference to the Biological Sciences*, New York, 1960.
- [43] S.L. Cymit química, Product categories: 6,6,7,7,8,8,8-Heptafluoro-2,2-dimethyloctane-3,5-dione, Cymit Química. (2023). <https://cymitquimica.com/products/TR-H069520/17587-22-3/6677888-heptafluoro-22-dimethyloctane-35-dione/> (accessed July 19, 2023).
- [44] S.L. Cymit Química, Product categories: Dibenzoylmethane, Cymit Química S.L. (2023). <https://cymitquimica.com/products/TR-D422683/120-46-7/dibenzoylmethane/> (accessed July 19, 2023).
- [45] S.L. Cymit Química, Product categories: Tri-n-octylphosphine Oxide, Cymit Química S.L. (2023). <https://cymitquimica.com/products/3B-T0504/78-50-2/tri-n-octylphosphine-oxide/> (accessed July 19, 2023).
- [46] S.M. Alshuaib, M.A. Al-Ghouti, Development of a novel tailored ion-imprinted polymer for recovery of lithium and strontium from reverse osmosis concentrated brine, *Sep. Purif. Technol.* 295 (2022), <https://doi.org/10.1016/j.seppur.2022.121320>.